



HAL
open science

An integrated framework to model nitrate contaminants with interactions of agriculture, groundwater, and surface water at regional scales: The STICS–EauDyssée coupled models applied over the Seine River Basin

Ahmad Tavakoly, Florence Habets, Firas Saleh, Zong-Liang Yang, Cyril Bourgeois, David R. Maidment

► To cite this version:

Ahmad Tavakoly, Florence Habets, Firas Saleh, Zong-Liang Yang, Cyril Bourgeois, et al.. An integrated framework to model nitrate contaminants with interactions of agriculture, groundwater, and surface water at regional scales: The STICS–EauDyssée coupled models applied over the Seine River Basin. *Journal of Hydrology*, 2019, 568, pp.943-958. 10.1016/j.jhydrol.2018.11.061 . hal-02313591

HAL Id: hal-02313591

<https://hal.sorbonne-universite.fr/hal-02313591v1>

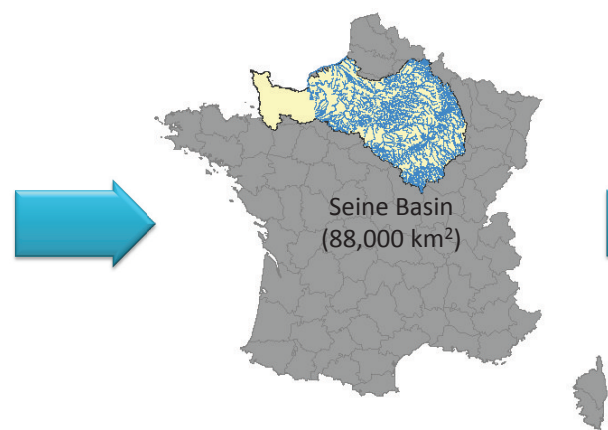
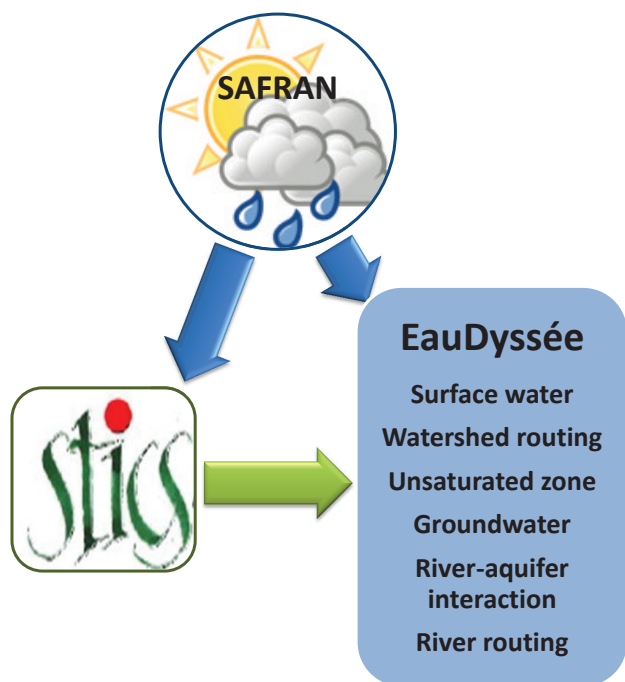
Submitted on 11 Oct 2019

HAL is a multi-disciplinary open access archive for the deposit and dissemination of scientific research documents, whether they are published or not. The documents may come from teaching and research institutions in France or abroad, or from public or private research centers.

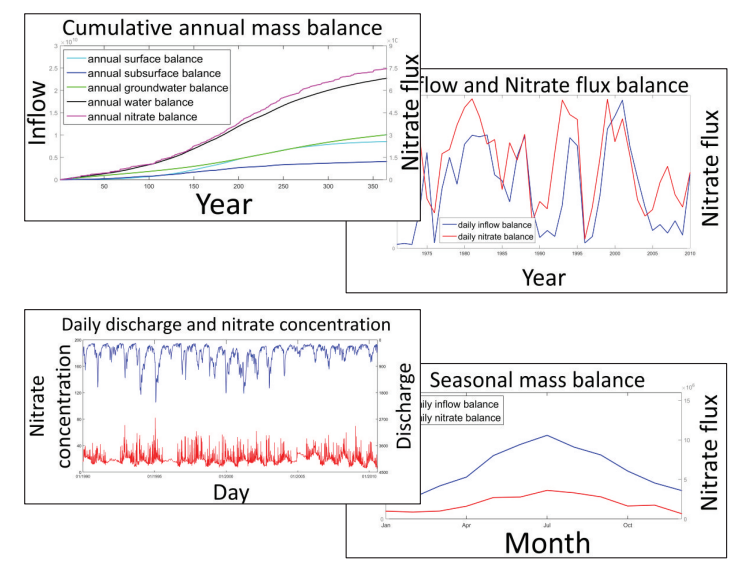
L'archive ouverte pluridisciplinaire **HAL**, est destinée au dépôt et à la diffusion de documents scientifiques de niveau recherche, publiés ou non, émanant des établissements d'enseignement et de recherche français ou étrangers, des laboratoires publics ou privés.

1
2
3
4
5
6
7
8
9
10
11
12
13
14
15
16
17
18
19
20
21
22
23
24
25
26
27
28
29
30
31
32
33
34
35
36
37
38
39
40
41
42
43
44
45
46
47
48
49
50
51
52
53
54
55
56
57
58
59
60
61
62
63
64
65

**An Integrated Framework to Model Nitrate Contaminants
with Interactions of Agriculture, Groundwater, and Surface
Water at Regional Scales: The STICS–EauDyssée Coupled
Models Applied over the Seine River Basin**



Products:
Time series of discharge, water elevation, and nitrate concentration
Basin-wide Water and Nitrate Balances



***Highlights (for review : 3 to 5 bullet points (maximum 85 characters including spaces per bullet point)**

Highlights

- Agronomic and distributed hydrologic models were coupled considering aquifer and river interaction
- Daily nitrate flux and riverine concentration were simulated for 39 years
- Simulated nitrate flux depends on the inflow produced by surface and subsurface
- Regional hydrologic modeling improves estimation of nitrate concentration
- Nitrate load to rivers increased during wet season and decreased during dry season

1 **An Integrated Framework to Model Nitrate Contaminants**
2 **with Interactions of Agriculture, Groundwater, and Surface**
3 **Water at Regional Scales: The STICS–EauDyssée Coupled**
4 **Models Applied over the Seine River Basin**
5

6 Ahmad A. Tavakoly*

7 Research Hydraulic Engineer, U.S. Army Engineer Research and Development Center, Coastal
8 and Hydraulics Laboratory

9 Florence Habets

10 Sorbonne Universités, UPMC, Univ Paris 06, CNRS, EPHE, UMR 7619 METIS, Paris, France

11 Firas Saleh

12 Stevens Institute of Technology, Davidson Laboratory, Department of Civil, Environmental and
13 Ocean Engineering, Hoboken, NJ 07030, USA

14 Zong-Liang Yang

15 Department of Geological Sciences, Jackson School of Geosciences, The University of Texas at
16 Austin

17 Cyril Bourgeois

24 Centre International de Recherche sur l'Environnement et le Développement, Nogent-sur-Marne,
25 France

26 David R. Maidment

27 Department of Civil, Architectural, and Environmental Engineering, The University of Texas at
28 Austin
29

30

31 ***Corresponding author**

32 Ahmad A. Tavakoly, Ph.D.

33 5825 University Research Court, Colege Park, MD 20740

34 Ahmad.A.Tavakoly@erdc.dren.mil

35

36 **Abstract**

37 Nutrient enrichment from natural and anthropogenic activities is one of the major
38 environmental pollution stressors. Nitrogen is one of the main reasons for failure to achieve a
39 good quality for the groundwater bodies in river basins. This study presents an integrated
40 framework that couples an agronomic model (STICS) and a distributed hydro(geo)logic model
41 (EauDyssée) to estimate nitrogen fluxes in the hydrosystem at the regional scale. The EauDyssée
42 modeling framework was enhanced to include nitrate transport from soils to rivers via surface
43 runoff and the onwards transport from aquifers to rivers. Furthermore, an in-stream nitrate model
44 to simulate nitrate concentration in the river network was implemented in the framework. The
45 utility of the integrated framework was demonstrated on the Seine River Basin with an area of
46 88,000 km², a complex hydrosystem with multiple aquifers, and one of the most productive
47 agricultural areas in France that encompasses the megalopolis of Paris. The STICS-EauDyssée
48 framework was implemented for a long-term simulation covering 39 years (1971-2010).
49 Comparison of groundwater nitrate concentrations with observations showed an overall absolute
50 bias of less than 10 mg/l. Model results showed that simulated nitrate fluxes to rivers highly
51 depend on the inflow produced by surface and subsurface waters. Simulated in-stream nitrate
52 concentration also compared well with observations, particularly in the eastern region of the
53 Seine River Basin. In general, results showed that a long-term simulation of nitrate contaminant
54 with the combined STICS-EauDyssée system was satisfactory at the regional scale. This work
55 can benefit decision makers to formulate management strategies and Agri-environmental
56 measures to mitigate pollution from agricultural activities to the river system.

57

58 **Keywords:** Nitrate flux; Surface-aquifer interactions; Regional scale modeling; Seine River

59 Basin; Distributed hydrologic modeling; STICS

60

61 **1-Introduction**

62 Increasing nitrate concentration in surface water and groundwater is a major concern of
63 water quality protection and consequently water resources management (Hooda et al., 1997;
64 Kampas and White, 2003; Vitousek et al., 1997). Anthropogenic activities including food and
65 energy productions have greatly increased nitrogen creation by over a factor of 10 compared to
66 the late-19th century (Galloway et al. 2004). The excess nitrate causes eutrophication and
67 adverse environmental effects such as harmful algal blooms (growth of phytoplankton in a water
68 body), hypoxia (oxygen depletion), and reduction of fish and shellfish production (Oehler et al.,
69 2009; Sebilo et al., 2003; Spalding and Exner, 1993; Wade et al., 2005; Zhang and Schilling,
70 2005). Climate change also has impacts on water quality. Changes in water discharge, velocity
71 which controls the residence time, water temperature, and precipitation are climate change
72 factors which can enhance nutrients (Ducharne et al., 2007; Sinha et al., 2017). Increasing of
73 water temperature can intensify biological activity and consequently nutrients (Ducharne 2008).
74 Using 21 different CMIP5 (Coupled Model Intercomparison Project Phase 5, Taylor et al., 2012)
75 models, Sinha et al., (2017) showed that the amount of riverine total nitrogen load will be
76 increased by $19 \pm 14\%$ in the United States based on the precipitation changes. Therefore,
77 developing a predictive capability of modeling nutrients transport is imperative to understand the
78 effect of climate change, and human activities on nitrogen changes at regional and global scales.

79 Before releasing nitrogen to the surface water, soil and groundwater have capacity of
80 nitrogen retention (nitrogen removal, Grizzetti et al., 2015). Nitrogen retention can occur in the
81 soil through denitrification process at the water saturated condition. Nitrogen denitrification and
82 accumulation can also take place in aquifers at the anoxic condition (dissolved oxygen is
83 depleted in groundwater). Aquifer permeability may also affect residence time of nitrogen and

84 attenuation in groundwater. Accordingly, sustainable development and comprehensive water
85 management require the need for the full representation of nitrate contamination from the soil
86 surface to the unsaturated zone, groundwater, and rivers for the entire basin. In terms of nutrient
87 modeling at the regional scales, a few models are introduced. Soil and Water Assessment Tool
88 (SWAT) is a commonly-used semi-distributed, continuous-time watershed model that predicts
89 the impact of land management on water, sediment, and chemical yields in ungagged watersheds
90 (Arnold et al. 1999). The model has a limitation to account for all sources of nitrogen such as
91 atmosphere (Alexander et al. 2002) and to determine point sources of N-inputs (Kunkel et al.,
92 2017). STONE uses one-dimensional physical based model to simulate N and P fluxes in
93 surface and groundwater and vertical transport of N between saturated and unsaturated top-soil
94 layers (Wolf et al., 2005). This model was used to analyze the impact of farming practices and to
95 evaluate environmental policies on nutrient emission over the Netherlands. MIKE SHE is a fully
96 distributed model and uses numerical solutions while solving the flow equations. As a
97 consequence, the model is computationally expensive and hence not adequate for large
98 watersheds (Borah and Bera 2003; Daniel et al. 2011). Other models such as the GROWA-
99 DENUZ-WEKU model system uses six diffuse input pathways (erosion, drainage system,
100 interflow, groundwater, wash-off, and atmospheric deposition) to determine the N input into
101 groundwater and surface water (Kunkel et al., 2004). This model is the most common model
102 system used in Germany at the level of river basins and Federal States (Kunkel et al. 2017;
103 Kunkel and Wendland 1997, 2002). The GROWA component of this model system uses
104 empirical approach to calculate long-term availability of water resources. To reduce the
105 computational cost, the GROWA model uses coarse temporal resolution (≥ 1 year) for climatic
106 input data (Kunkel and Wendland 2002).

107 Considering the interactions of surface water and groundwater is vital to understand nitrate
108 changes in the hydrosystem (Baratelli et al., 2016). Flipo et al., 2014 conducted an extensive
109 literature review of distributed physically based models. According to their study, only 19 of 183
110 publications were at the regional scale ($> 10,000 \text{ km}^2$) where two of them considered stream-
111 aquifer exchanges (Monteli, 2011 and Pryet et al., 2015). Moreover, Baratelli et al., (2016)
112 showed that considering the river stage fluctuations improve the accuracy of the discharge
113 modeling and the assumption of constant river stage can result to a significant underestimation of
114 total infiltration and exfiltration at the regional scale. The sensitivity study was conducted using
115 the EauDyssée platform (Pryet et al., 2015; Saleh et al., 2011) in their study. This platform
116 includes in-stream water level fluctuations and an explicit quantification of the stream-aquifer
117 exchanges.

118 The research proposed herein incorporates hydrological modeling system and agronomic
119 model to improve understating of the nutrient dynamics in surface water and groundwater
120 interaction and in streams over large scale river networks and long-term time periods. For this
121 purpose, the EauDyssée platform with its unique aforementioned capabilities was applied and
122 developed to simulate nitrate contaminants. Coupling of the EauDyssée model and the
123 agronomic model STICS (Simulateur mulTidisciplinaire pour les Cultures Standard, Beaudoin et
124 al., 2016; Brisson et al., 1998, 2002), to obtain the infiltrating nitrate flux leaving the root zones
125 is presented. Furthermore, this study shows the application of streamflow results from a large
126 scale river routing model to simulation nitrate at the regional scale. The modeling system was
127 implemented over the Seine River Basin in France. Due to increasing nitrate concentrations over
128 time, the Seine River Basin represents an ideal test bed of river nutrient chemistry in a regional
129 ecosystem. In 2013, most of the surface and groundwater bodies of the Seine River Basin did not

130 have such a desirable status, mostly due to nutrients in the groundwater bodies (AESN, 2013).
131 Nutrient enrichment and eutrophication are major environmental phenomena in the French
132 coastal zone. Many studies have investigated the nitrogen cycle of the Seine River Basin with
133 different purposes. Some studies focused on the nutrient transfers for a portion of or the entire
134 Seine River Basin, but did not explicitly include stream-aquifer interaction (Billen et al., 2007;
135 Cugier et al., 2005; Even et al., 2007; Garnier et al., 2005; Passy et al., 2012; Sebilou et al., 2003;
136 Sferratore et al., 2005; Thieu et al., 2009, 2010). Other studies only considered the aquifers
137 (Bourgois et al., 2016; Ledoux et al., 2007; Philippe et al., 2011; Viennot, 2009), and some
138 complete studies only encompassed smaller parts of the Seine River Basin (Flipo et al., 2007a;
139 2007b), which can support the understanding of nutrient transformations.

140 This study describes simulation of nitrate flux leaching into the river network and
141 consequently to compute in-stream nitrate concentration for the entire Seine River Basin,
142 including several layers of aquifers over 39 years (1971-2010). Transport of nitrate from land to
143 rivers and from aquifers to surface water and rivers were added to the EauDyssée platform.
144 Taking the leaching nitrate from EauDyssée and streamflow simulations, first order solute
145 transport model was also developed to simulate in-stream nitrate concentration at the regional
146 scale. The new enhancements allow the EauDyssée platform to simulate regional watershed flow
147 and solute modeling with stream and aquifer interactions.

148 **2- Materials and Methods**

149 **2-1-Study Area**

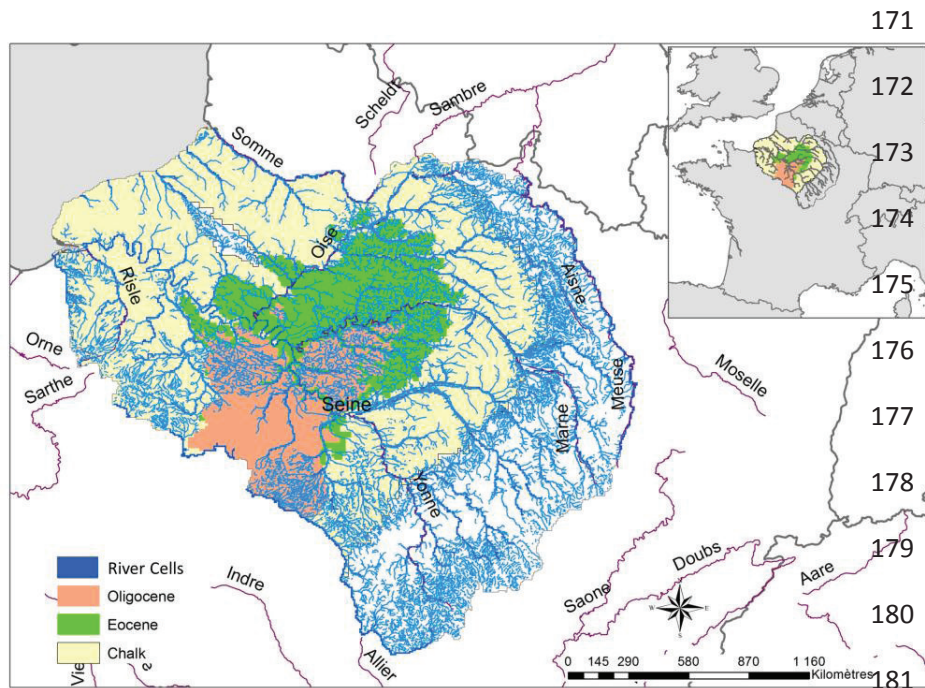
150 The Seine River Basin covers an area of approximately 88,000 km² in northern France
151 (Figure 1). The Seine River is 776 km long and has 25,000 km of tributaries (Table 1). It begins

152 at an elevation of 446 m at Source-Seine in the department of Côte-d'Or in Burgundy and
 153 discharges into the English Channel near the city of Le Havre. Table 1 shows that the stream
 154 gradients are not extremely varied; although elevation ranges from 0 to 856 m above sea level,
 155 with 90% of the basin is below 300 m. The hydrological regime of the Seine River Basin is
 156 considered to be pluvial oceanic, with varied seasonal flows (high flows in winter and low flows
 157 in summer) that reflect rainfall distribution throughout the year. The Seine River Basin also has
 158 several aquifers that play an important role in sustaining base flow (Rousset et al., 2004).
 159 Interactions of three major aquifers with the river network were considered in this study. These
 160 aquifers are from top to bottom: 1) Oligocene; 2) Middle and lower Eocene; and 3) Upper-
 161 Cretaceous chalk (Gomez et al., 2003b). The aquifers are relatively permeable (from medium to
 162 high), and are relatively vulnerable (from medium to high). The middle and lower Eocene is
 163 composed of coarse limestones of Lutetian and sands. The total transmissivity varies from 5 to
 164 10^{-4} m²/s. The Upper-Cretaceous chalk aquifer has a porosity between 37 and 45% and a
 165 transmissivity less than 10^{-2} m²/s. A full description of the Seine aquifers is available at
 166 <http://sigessn.brgm.fr/spip.php?rubrique5>.

167 **Table 1: Mean and total morphological characteristics of the Seine River Basin from the river**
 168 **network Carthage.**

Stream Order	Number	Mean		Total	
		Width (m)	Slope (m/m)	Length (km)	Catchment area (km ²)
1	2,887	2.5	0.0151	11,714	42,234
2	1,440	5.9	0.0062	5,591	17,190
3	848	12.6	0.0034	3,801	12,493
4	354	23.0	0.0022	1,932	6,982
5	186	50.2	0.0014	1,102	4,497
6	115	88.9	0.0013	601	2,416
7	36	200.9	0.0011	383	2,113
Entire Seine River Network	5,866	10.5	0.0097	25,124	87,926

169



182 **Figure 1: The Seine River Basin including the river network and its main aquifers.**

183

184 The Seine River Basin is predominantly covered by an intensive agricultural industry with
 185 up to 57% of the land surface allocated to agriculture (Mignolet et al., 2007), which is the main
 186 source of nutrients entering rivers in Europe (De Wit et al., 2002). The rest of the basin is
 187 covered by forest (25%), grassland (13%), and urban (5%). The center of the basin dominantly
 188 covered by cereal, oilseed, and sugar beet croplands. The outer limit of the basin is mostly
 189 covered by forest and grassland (Garnier et al., 2009; Sferratore et al., 2005). The Seine River
 190 Basin is home to approximately 20 million inhabitants, including 10 million people in the region
 191 of Paris. Agricultural activity, pollution sources, and population density lead to water quality
 192 degradation and nutrient enrichment of the Seine River Basin. Furthermore, this basin includes a
 193 major aquifer system made by a series of connected aquifer layers that interact with surface

194 water resources and are key components of the hydrological and biogeochemical processes of the
195 area (Contoux et al., 2013; Gomez et al., 2003b).

196 **2-2-Descriptions of Models**

197 This research is based on the coupling of an agronomic model, STICS, and a regional
198 hydrological model, EauDyssée over the entire Seine River Basin. The meteorological forcing
199 data for EauDyssée includes precipitation and potential evapotranspiration which are produced
200 by a mesoscale atmospheric analysis system, Météo-France SAFRAN (Durand et al., 1993;
201 Quintana-Seguí et al., 2008), at a daily time step over a regular 8-km grid.

202 *2-2-1-The STICS Crop Model*

203 STICS (Brisson et al., 2003) is a process-based daily time step crop model that simulates
204 (a) crop yields in terms of quantity and quality and (b) the environment in terms of drainage and
205 nitrate leaching. STICS is able to: adapt to various crops using the same set of equations and
206 specific parameters, simulate various climate and soil conditions, add new modules, and
207 communicate externally with other models and developers. The input variables are related to
208 climate, soil, and the crop system (Schnebelen et al., 2004). The upper boundary corresponds to
209 climatic variables including solar radiation, daily minimum and maximum temperatures,
210 precipitation, and reference evapotranspiration. The lower boundary corresponds to the soil/sub-
211 soil interface. The core of the STICS model includes four primary sets of modules. The first set
212 of modules includes phenology, shoot growth, and yield formation. This set considers the
213 ecophysiology of aerial plant parts. The second set contains four modules (root growth, water
214 balance, nitrogen balance, and soil transfer) that simulate the interaction between underground
215 plant parts and soil functions. The third module is crop management, which accounts for water
216 transfer through the canopy, the status of water and heat balances in the soil-crop system, and

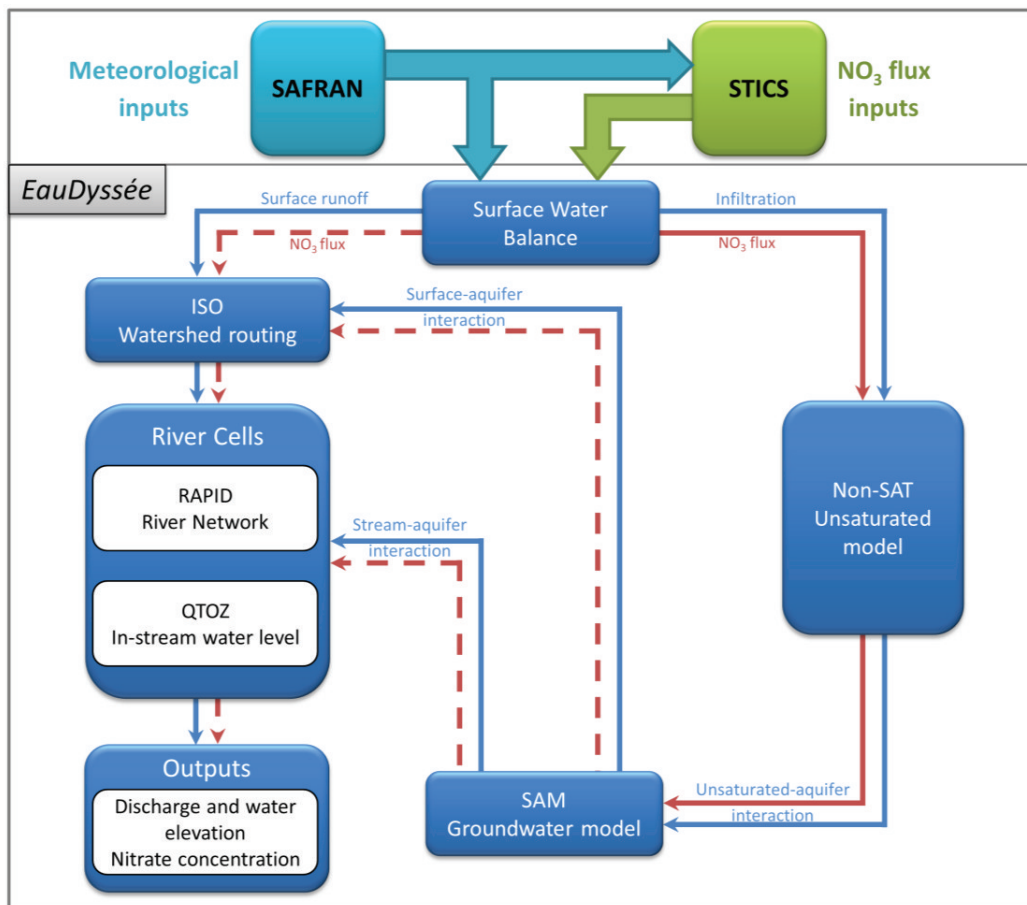
217 fertilizers. The fourth module is the microclimate, which calculates temperature and air humidity
218 through the canopy.

219 Three principal databases are used in the STICS model to characterize the pedology,
220 meteorology, and agriculture of the Seine River Basin. The three databases are: soil, agriculture,
221 and meteorological; each has a different spatial resolution (Beaudoin et al., 2016; Ledoux et al.,
222 2007). The intersection of these databases generates spatial units called General Simulation Units
223 (GSU) that share the same spatial, pedological, agricultural, and meteorological characteristics.
224 STICS was made up of 9596 units with an average unit area of 12 km² over the Seine River
225 Basin. The dominate nitrogen process in the Seine Basin is nitrate due to the majority covering
226 of the landscape with clear-cut forest and agricultural system (Billen et al., 2007). Consequently,
227 The STICS model has been extensively used as an agronomical model in this basin. The nitrogen
228 flux estimated by STICS on the Seine River Basin was recently assessed by Beaudoin et al.,
229 2016.

230 *2-2-2-The EauDyssée Platform*

231 The EauDyssée modeling platform is a hydrometeorological and biogeochemical model
232 based on the existing models and databases of the PIREN-Seine program. The hydrogeological
233 component of the model uses the same principles as the MODCOU model (Habets et al., 2008;
234 Ledoux et al., 1989). EauDyssée couples existing specialized modules to simulate water
235 resources (quantity and quality) at regional scales (Figure 2): the surface component, the river
236 routing component, the unsaturated component, and the groundwater dynamic or saturated
237 component (Philippe et al., 2011; Pryet et al., 2015; Saleh et al, 2011).

238
239
240
241
242
243
244
245
246
247
248
249
250



251 **Figure 2: Schematic representation of coupling among SAFRAN, STICS, and EauDyssée. The solid blue line represents an existing coupling system between modules for flow simulations in the**
 252 **EauDyssée platform. The solid red line shows an existing NO₃ flux simulation from surface to Non-**
 253 **SAT and from Non-SAT to the SAM groundwater model prior to this study. The dashed red line**
 254 **represents NO₃ flux simulation added in this study.**
 255

256 The surface component of EauDyssée uses a seven-parameter conceptual model to
 257 compute water mass balance at a daily time step for each cell of the surface mesh (Deschesnes et
 258 al., 1985). In this module, the domain is divided into units called production functions that are
 259 generated based on the interaction of land-use and geological units (Golaz-Cavazzi et al., 2001;
 260 Gomez et al., 2003a). Inputs to the surface component are precipitation and potential
 261 evapotranspiration with a daily time step provided by SAFRAN. The outputs are actual
 262 evapotranspiration (AET), surface runoff, infiltration, and soil storage. The total number of

263 surface cells covering the Seine River Basin is 35,698 with an average resolution of one square
264 kilometer. The ISO module is used to route surface runoff to the river network. A number of
265 isochronal zones, representative of the number of travel time steps, are defined in the ISO
266 module to determine the delay between runoff generation and the time that runoff reaches the
267 nearest river cell.

268 EauDyssée incorporates a river network model called Routing Application for Parallel
269 Computation of Discharge (RAPID) in the river network component (David et al., 2011b) and a
270 module to estimate river water level fluctuation called QtoZ (Saleh et al., 2011). Inclusion of
271 RAPID allows a direct computation of flow for each river cell of the quad tree river network and
272 flexibility in the number and location of river gages. The QtoZ module improves river-aquifer
273 interaction by taking into account river water level fluctuations. Application of the RAPID model
274 in the SIM-France model was discussed by David et al. (2011a). The RAPID model has been
275 extensively applied in the United States (e.g. David et al., 2013; Follum et al., 2016; Tavakoly et
276 al., 2012, 2016a, 2016b). Inputs to RAPID are surface and subsurface runoff generated by the
277 ISO module, and outputs are streamflow in each cell of the grid river network. Discharge
278 computed by RAPID is used by the QtoZ module to calculate water levels at a given river cell in
279 the EauDyssée platform. At each time step QtoZ computes a water level that is sent to the
280 groundwater model (SAM) to simulate stream-aquifer interactions. QtoZ has three options for
281 calculating water levels: (a) fixed water level, (b) rating curve, and (c) the Manning equation.
282 Taking streamflow simulated by the RAPID model, the Manning equation option was modified
283 in this project to estimate flow velocity and cross-sectional area for each river cell at every time
284 step.

285 Infiltration is vertically portioned by the production function transferred to groundwater
286 within the unsaturated zone. The unsaturated zone component, NONSAT (Ledoux et al., 1989),
287 consists of Nash reservoir cascade (Nash, 1960). The number of reservoirs depends on the
288 distance between soil horizons and the saturated zone, which is initially calculated on the basis of
289 hydraulic head distribution. Prior to this study, NONSAT was adapted to transfer solute
290 components (Gomez et al., 2003a; Philippe et al., 2011).

291 The groundwater component SAM (Simulation of Multilayer Aquifers) is a regional
292 spatially-distributed model that applies the diffusivity equation to compute both the temporal
293 distribution of hydraulic heads and the flow in multilayer aquifer units (Ledoux et al., 1989;
294 Marsily, 1986). SAM computes the water flux exchanged between aquifer and stream grid-cells
295 using water levels calculated by the QtoZ module and river volumes calculated by RAPID. SAM
296 also simulates the diffusive transfer of passive solute (Bourgeois et al., 2016; Ledoux et al.,
297 2007; Philippe et al., 2011). The three aquifers version of the EauDyssée platform was first
298 established by Gomez et al., (2003b). The model was previously used to study climate change
299 impact on the rivers and groundwater (Habets et al., 2013). Assessment was based on over 130
300 wells, with a bias lower than 1m for fifty percent of them. In this study, the EauDyssée platform
301 was enhanced so that contaminants such as nitrate can be routed to the river. Improvements are
302 explained in the following section.

303 *2-2-3-Developments in the EauDyssée Platform to Simulate Surface and Stream-Aquifer Nitrate* 304 *Exchange*

305 Developments of the nitrate simulation in this study are illustrated with dashed red in
306 Figure 2. The solute transport was added to watershed routing within the surface component of
307 the EauDyssée platform. The ISO module (Figure 2) routes runoff to the river network with the
308 association of the isochronal zones. The ISO module is modified to accumulate the mass of

309 solute constituents and define the total mass transferred to river cells. A new module called “ISO
 310 solute”, was added to the EauDyssée platform to model watershed solute transport and to provide
 311 nitrate flux leaching to river cells. The ISO solute module has the advantage of including the
 312 solute flux received from the aquifer in addition to the solute transport from surface runoff. The
 313 solute transport with the stream-aquifer interaction was developed based on the approach used to
 314 simulate stream-aquifer exchange flow in the EauDyssée platform. The flow exchange between
 315 the stream and the aquifer is computed based on the difference of hydraulic heads for river cells
 316 and associated aquifer cells (Rushton, 2007):

$$317 \quad Q_r = R_C \times (h_r - h_p) \quad (1)$$

318 where Q_r is the stream-aquifer flow (L^3T^{-1}); R_c is the hydraulic conductance of the stream-
 319 aquifer interconnection (L^2T^{-1}); h_r is the water elevation of the stream(L); and h_p is the
 320 piezometric head in aquifer (L).

321 Two different directions for stream-aquifer exchange flow are considered for each river
 322 cell at each time step: flow from the *aquifer to river* ($Q_{A \rightarrow R}$) and flow from *river to aquifer* (
 323 $Q_{R \rightarrow A}$). The majority of streams in the Seine River network are gaining streams with the net
 324 aquifer-to-stream flow values between 0 and $+0.1 \text{ m}^3/\text{s}$, which means the aquifer system supplies
 325 the river network and only few river reaches are losing flow to the aquifer (Pryet et al. 2015).
 326 Based on this fact, the assumption was that the transfer of constituent to the aquifer from river is
 327 negligible. Therefore, $Q_{A \rightarrow R}$ is used in the stream-aquifer solute modeling. Nitrate load
 328 transported by aquifer is calculated by multiplying both sides of equation (1) by a nitrate
 329 concentration:

$$330 \quad L_{A \rightarrow R} = C_x \times R_C \times (h_r - h_p) \quad (2)$$

331 where $L_{A \rightarrow R}$ is the nitrate load transported by *aquifer to river* flow (MT^{-1}); and C_x is the nitrate
332 concentration (ML^{-3}), which is provided based on the coupling of EauDyssée and STICS.

333 As a final model outputs of the modeling framework, the in-stream nitrate concentration
334 (with the unit of mg/l) was simulated by the first order decay rate for entire river network. This
335 approach has been extensively applied to study nutrient study at the basin scale (e. g. Liu et al.,
336 2008, Runkel 2007; Smith et al., 1997; Tavakoly et al., 2016a). The decay rate (k) was
337 determined based on the uptake length and the stream velocity:

$$338 \quad k = \frac{V}{S_w} \quad (3)$$

339 where: V is the stream velocity (LT^{-1}) and S_w is the uptake length (L).

340 Using the RAPID streamflow simulations, time series of the stream velocity for all river
341 cells was computed by the QtoZ module. The range of S_w is defined based on the stream order.
342 Using the predefined range in Table 2 (Ensign and Doyle, 2006), the uptake length is determined
343 for river cells through the calibration procedure. The k coefficient was then calculated for all
344 river cell and time steps.

345 *2-2-4-Limitation of Modeling Framework*

346 In terms of framework limitations, STICS model computes the full nitrogen cycle within
347 the upper soil, and the amount of leaching nitrogen (Brisson et al., 2003). Once leached, only the
348 convection is taken into account, both in the unsaturated and saturated zones, with time transfer
349 varying according to the characteristics of each grid cell. Therefore, there is no nitrification,
350 denitrification nor mineralization once the nitrogen has left the soil column. This is the reason
351 why a decay rate is considered. The decay rate is varied according to the stream order of the river
352 cell, which is explained in the following section. Additionally, the modeling chain include

353 drainage (downward flux in the soil associated to gravity). However, it doesn't include a special
354 treatment for those agricultural area that are drained using artificial pipe, because the data to
355 account for it at the basin scale are not available.

356 *2-2-5-Calibration Process*

357 Calibration of the nitrate concentration in the river network was conducted manually using
358 daily nitrate concentration over the period 1995-2000. The uptake length (S_w) was optimized
359 using three objective functions: Root Mean Square Error (*RMSE*), Correlation Coefficient (ρ),
360 and Kling–Gupta Efficiency (*KGE*, Gupta et al., 2009). The strength of *KGE* is to optimize
361 solution from the three-dimensional criteria space considering correlation, variability, and bias,
362 which is an explicit component in this performance metric (Bennett et al., 2013; Haas et al.,
363 2016). The parameter S_w was adjusted within the defined range in Table 2 by trial and error to
364 obtain maximum ρ and *KGE* and minimum *RMSE*. Once the optimized S_w is obtained, the
365 decay rate (k) was calculated using equation (3). This method allows determination of a
366 temporal variation of k (daily scale), since the velocity varies with time in equation (3). The
367 optimized S_w was then assigned to river cells around each station. Moreover, lower and upper
368 bands, 4×10^{-5} and 1×10^{-3} (s^{-1}) for k , were contemplated in this study (Faulkner and Campana,
369 2007; Runkel, 1998). The optimized S_w and temporal averages of k for different stream orders
370 are shown in Table 2.

371

372

373

374

375 **Table 2: Range of S_w and summary of calibration results for S_w and k .**

Stream Order	Range		Mean
	S_w (m)	S_w (m)	k (s ⁻¹)
≤ 3	84-996	610	0.000912
4-5	119-1006	930	0.000530
≥ 6	170-4915	1961	0.000270

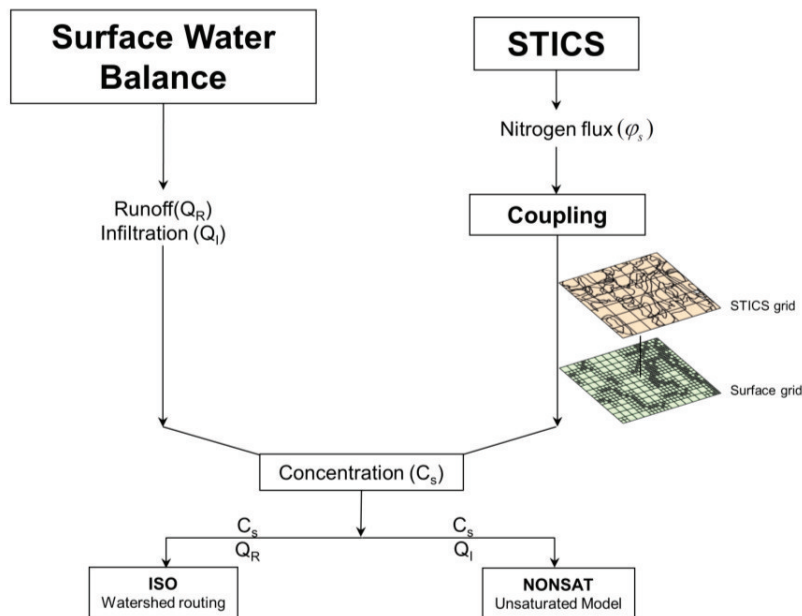
376 The magnitude of the obtained S_w and k values in this study is in the same order of
 377 published values ($S_w = 671$ m and $k = 1.5 \times 10^{-3} \text{ s}^{-1}$) by Klocher et al., (2009), which was a study
 378 on rivers with stream order less than three.

379 **2-3-Modeling Framework Applied to the Seine River Basin**

380 Following the same methodology as in Beaudoin et al., 2016, the EauDyssée and STICS
 381 models were coupled for nitrogen transport simulation in the Seine River Basin for a long-term
 382 period (from August 1, 1971, to July 31, 2010). The schematic framework for the spatial
 383 coupling of EauDyssée and STICS was displayed in Figure 3. The first step in superimposing
 384 EauDyssée was to calculate nitrate flux for each surface cell. GIS was utilized to determine the
 385 spatial contribution of nitrate flux to surface cells. The intersect tool in ArcGIS is applied to
 386 correlate corresponding GSUs to the surface cells and to compute the areal proportion of the
 387 GSU that overlaps with the surface cells. In the second step, nitrate flux (STICS output) was
 388 diluted by runoff and infiltration for each surface cell with the assumption of both having the
 389 same concentration:

$$390 \quad C_s = \frac{\varphi_s}{Q_R + Q_I} \quad (4)$$

391 where C_s and φ_s are the nitrate concentration (ML^{-3}) and nitrate flux (M) at each surface cell;
 392 Q_R and Q_I are daily runoff and infiltration (L^3).



393

394 **Figure 3: Schematic representation of the spatial coupling of EauDyssée and STICS.**

395 Runoff and infiltration are calculated by the surface water balance component of
 396 EauDyssée. Once the nitrate concentration was calculated for all 35,698 surface cells at all time
 397 steps in the study period, the solutes were transferred through the unsaturated zone, groundwater
 398 and routed by EauDyssée to river cells at a daily time steps. The results for the hydrologic and
 399 hydrogeological components of the framework builds on previous results carried out by Philippe
 400 et al., (2011), Pryet et al., (2015), Saleh et al., (2011). In their work, the EauDyssée streamflow
 401 results were calibrated and validated by comparing simulations to measurements at 118 gages
 402 within the Seine River Basin (Pryet et al., 2015). The simulated flows were then used to compute
 403 daily nitrate concentration for 6,481 river cell covering the Seine River Basin in this study. Using
 404 the first order uptake, the daily nitrate concentration was then computed by routing the mass

405 from upstream to downstream in the river network from 1971 and 2010. Daily riverine nitrate
406 concentration was simulated for 6,481 river grid-cells of which 3,519 interacted with aquifers
407 (Figure 4).

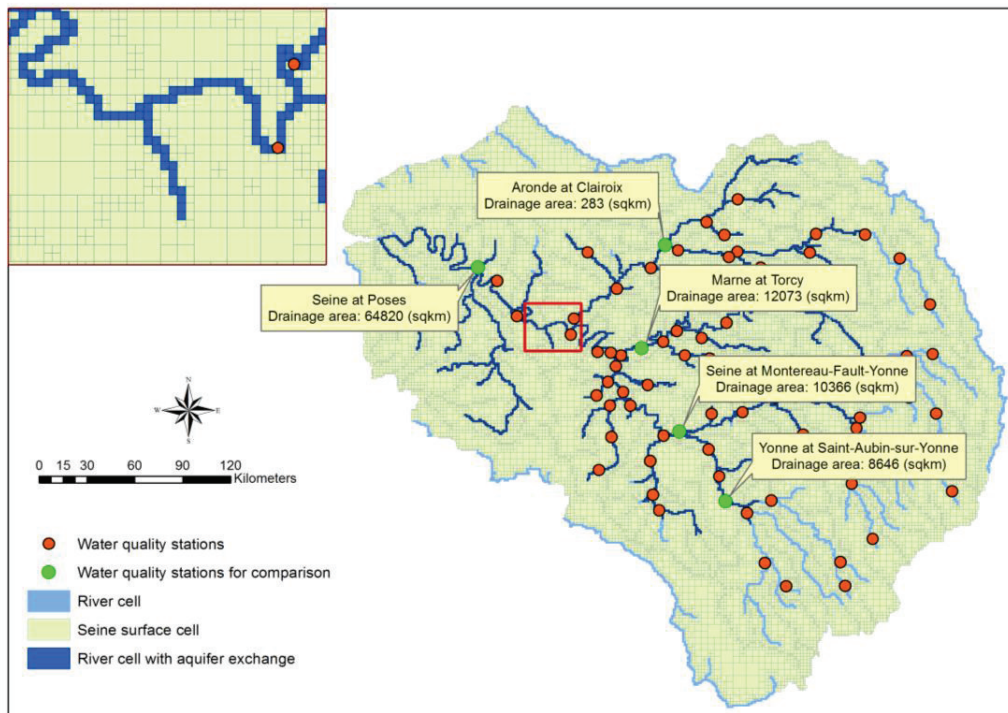
408 *2-3-1-Groundwater initialization*

409 To compare observed and simulated groundwater nitrogen concentrations, special attention
410 was paid to the setting of the initial condition. Indeed, the time transfer in the unsaturated zone
411 can last more than 30 years (Philippe et al., 2011). To set the initial concentration, three periods
412 with different nitrogen leaching concentration were considered with the EauDyssée runs: the first
413 period is pre-industrial (before 1935), and considered that the lixiviated nitrogen can be similar
414 to the one from current organic farming. According to Thieu et al., (2010), a homogeneous
415 concentration of 26mg/L was used. Such forcing data was repeated long enough and the
416 EauDyssée was run to reach a stable groundwater concentration. The results were then
417 comparable to the data collected by Landreau and Roux (1984) in 1930. The second period lasts
418 from 1935 to 1970. For this period, the nitrogen lixiviation was considered to increase linearly
419 between the pre-industrial value and the value estimated by STICS for the period of 1970-1971.
420 For the last period, the nitrogen leaching is estimated by STICS.

421 **2-4-Observation Data**

422 More than 6,000 wells monitoring the groundwater quality in the Seine River Basin are
423 available from the Accès aux Données sur les Eaux Souterraines (ADES) database
424 (<http://www.adès.eaufrance.fr/>). However, they cover different time periods and are not all
425 available for a given date. Observed river nitrate data were also used to evaluate and compare
426 modeling results. In total, 72 stations with more than 150 sampling dates were available between
427 1985 and 2010 (Figure 4). The selected water quality stations cover wide range of drainage area,

428 $O(100-10,000)$ km². Five of the water quality stations were selected to discuss comparison
 429 between daily time series of observed and simulated streamflow and nitrate concentration.
 430 Selected stations are shown with green colored dots in Figure 4. The Poses station, located
 431 downstream of Paris before the tidal influence, was used to assess the overall performance of the
 432 Seine River Basin model with the drainage area of 64,820 km² (Figure 4). The Aronde at
 433 Clairoix station is located in the northern part of the Seine River Basin with high agricultural
 434 activity. The Torcy station is located on the downstream of the Marne River, an eastern tributary
 435 of the Seine River Basin. The Montereau-Fault-Yonne station is on the Seine River which is
 436 located downstream of Troyes. The Saint-Aubin-Sur-Yonne station is located on the Yonne
 437 River, the southeast tributary of the Seine River.



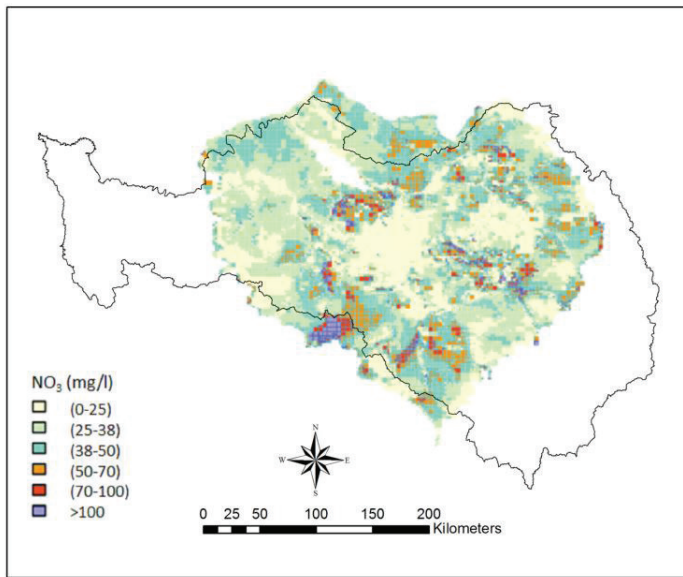
438
 439 **Figure 4: The EauDyssée river network and water quality stations used in this study with their**
 440 **respective drainage areas.**

441 **3-Results and Discussion**

442 This section covers three topics: evaluation of the nitrate concentration in groundwater,
443 comparison of the annual inflow and nitrate flux, and evaluation of the in-stream nitrate
444 concentration. The EauDyssée platform was run at a daily time step for the groundwater
445 modeling and at the 30-minute time step for the streamflow modeling to simulate daily nitrate
446 flux over 39 years (1971-2010).

447 **3-1-Comparison of Simulated and Observed Nitrate Flux in Groundwater**

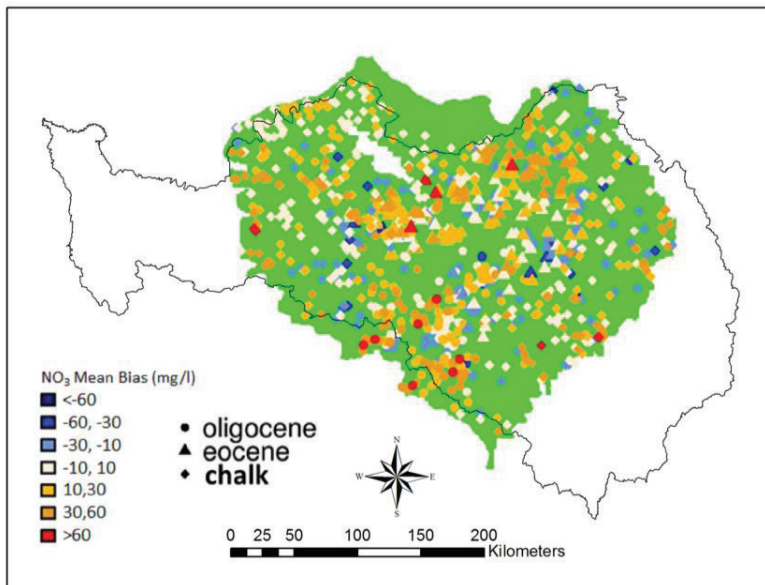
448 Following the method described in the section 2-3-1, the evolution of the groundwater
449 concentration compared quite well with the observations (Figure 5). The map shows that the
450 concentration is above the 50 mg/L target threshold in many parts of the aquifers. Figure 6
451 presents the mean bias between the observed and simulated concentration during the period
452 1970-2010 ($\text{Bias} = \overline{C_{\text{simulated}} - C_{\text{observed}}}$). It appears that the absolute bias is less than 10mg/L
453 on average. The large bias (bias > 30 mg/l) was found in the northern tributary of the Seine River
454 (Oise River). This could be explained by the fact that the hydrogeology model is less
455 representative in this part of the Seine River Basin (Pryet et al., 2015). Beaudoin et al., 2016
456 showed that the overestimation of lixiviated nitrogen could occur in this area due to an
457 underestimation of the yield by the STICS model. Figure 7 presents the temporal evolution of the
458 observed and simulated nitrogen concentration on average on the 3 aquifer layers. The method
459 used to initialize the nitrogen concentration in groundwater is able to provide a nitrate
460 concentration comparable to the observations at the beginning of the simulated period (1970),
461 except for the Oligocene. From 1970 to 2010, the simulation reproduces quite well the increase
462 in nitrate concentration in Chalk, the largest aquifer, underestimates in the Eocene and ends with
463 a concentration close to observations in the Oligocene



464

465 **Figure 5: Average concentration of groundwater nitrate in 2010.**

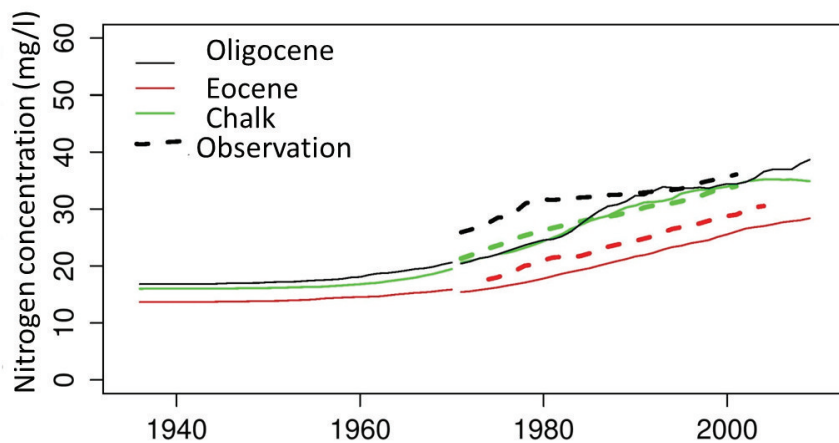
466



467

468 **Figure 6: Spatial distribution of the mean bias between observed and simulated nitrate**
 469 **concentration, with the distinction of the 3 aquifer layers (note that the gage can be in a confined**
 470 **part of the aquifer).**

471



472

473 **Figure 7 Temporal evolution of the mean observed and simulated nitrogen concentration in the**
 474 **three aquifer layers.**

475

476 **3-2-Comparison of Annual Average for the Simulated Inflow and Nitrate Flux**

477 Nitrate fluxes leaching to rivers are carried by surface runoff and groundwater. To better
 478 understand nitrate delivery, the annual average of nitrate flux was compared with annual average
 479 of inflow to river cells (Figure 8). Results show that the amount of nitrate delivered to river cells
 480 is highly dependent on inflow. The amount of leaching nitrate is low during the dry years, and
 481 increases during the wet years, which is consistent with having more leaching in the wet years
 482 than the dry years. For example, the lowest amount of nitrate was delivered in 1996 and 1997 at
 483 the Poses station, while the annual average of inflow in these years was 173 and 382 m³/s,
 484 respectively. In contrast, in wet years, the annual average is significantly increased. The model
 485 outputs show that 2000 and 2001 were characterized by very high discharge rates. The delivered
 486 nitrate was also increased for these years. In general, low nitrate load was delivered to rivers in
 487 1976, 1985, 1990-91, 1996, and 2005-06, which were characterized as dry years. On the other
 488 hand, high amount of nitrate was delivered to rivers in 1988, 1993, 2000, and 2001. These years
 489 had a high discharge and were categorized as wet years. The increasing of nitrate during wet

490 years can be explained by the effect of rainfall. During wet years, the heavy rain causes
 491 accumulation of rainfall and raising the water table which will increase the storage of nitrogen in
 492 the shallow soil layers and subsequently, more nitrate is transported to rivers. During the dry
 493 year, the amount of nitrate inclines to develop, due to the low uptake rate by plants, and it will
 494 flow to river network during the following wet years. Unlike other stations, the nitrate load
 495 leaching to the river cells failed to follow the inflow variation at the Saint-Aubin-sur-Yonne
 496 station (Figure 8). This is likely due to the negligible effect of the groundwater in this area where
 497 the nitrate load is primarily the surface load.

498

499

500

501

502

503

504

505

506

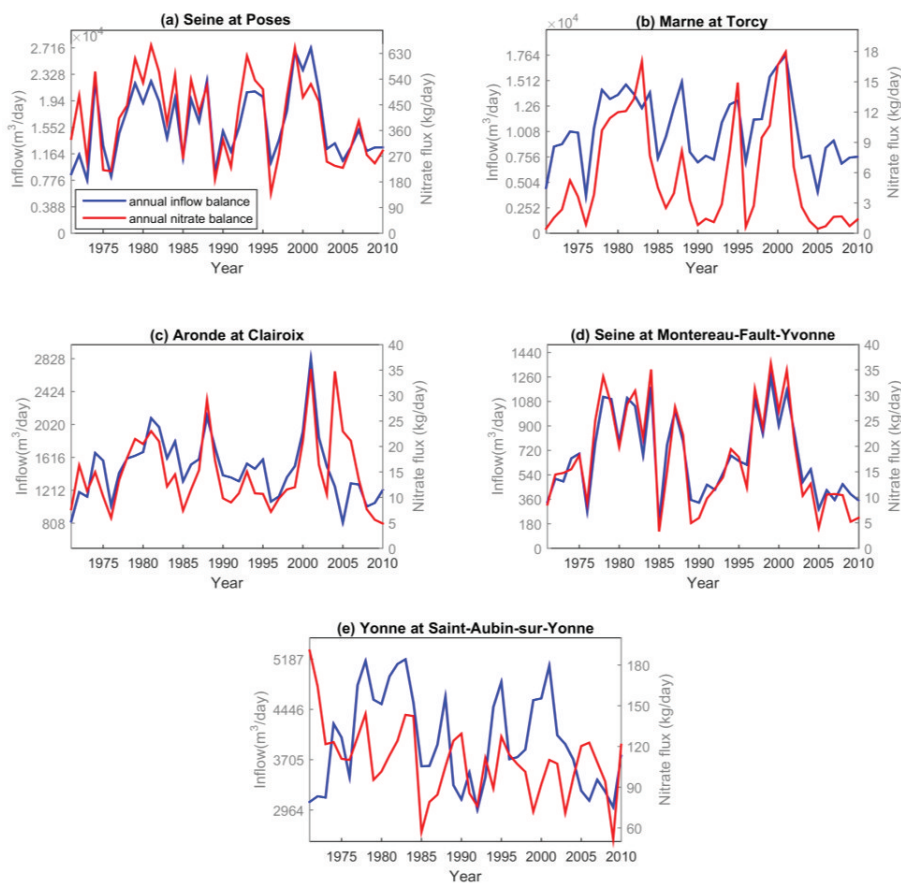
507

508

509

510

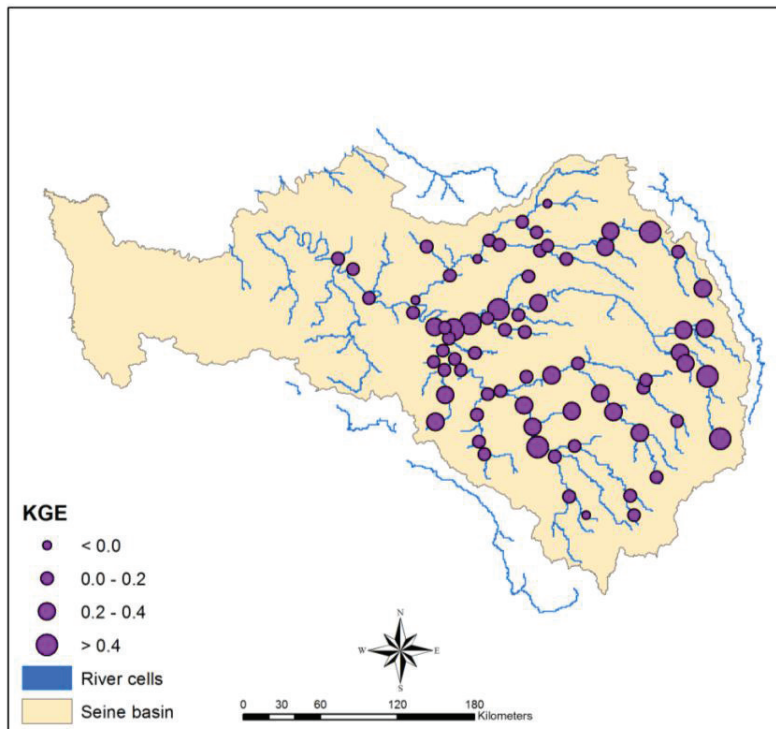
511



512 **Figure 8: Simulated annual average nitrate flux and inflow for the selected stations: (a) Seine at**
 513 **Poses; (b) Marne at Torcy; (c) Aronde at Clairoix; (d) Seine at Montereau-Fault-Yonne; and (e)**
 514 **Yonne at Saint-Aubin-sur-Yonne.**

515 **3-3-Simulation of In-stream Nitrate Concentration**

516 Figure 9 shows the *KGE* values of in-stream nitrate simulations for all stations in this
517 study. The daily *KGE* was calculated using point-by-point concurrently comparison of observed
518 and simulated values. Observed nitrate concentrations are available from 1985 to 2010 for most
519 stations. The spatial distribution of *KGE* values demonstrated an overall satisfactory model
520 performance in terms of simulating long-term daily nitrate concentration. The *KGE* results
521 (Figure 9) indicate that the model performed relatively better in eastern regions of the Seine
522 River Basin compared to the west part of the basin. Clearly, Nitrate concentration strongly
523 depends on the hydrological simulation, which confirms findings from literature (Thieu et al.,
524 2009). A relatively poor performance of EauDyssée with regard to the hydrological simulation in
525 the western part of the basin can explain the reason (Pryet et al., 2015). Additionally, the
526 comparison of nitrate concentration in groundwater (Figure 6) shows relatively large bias in the
527 northwestern tributary of the Seine River Basin (Oise River).

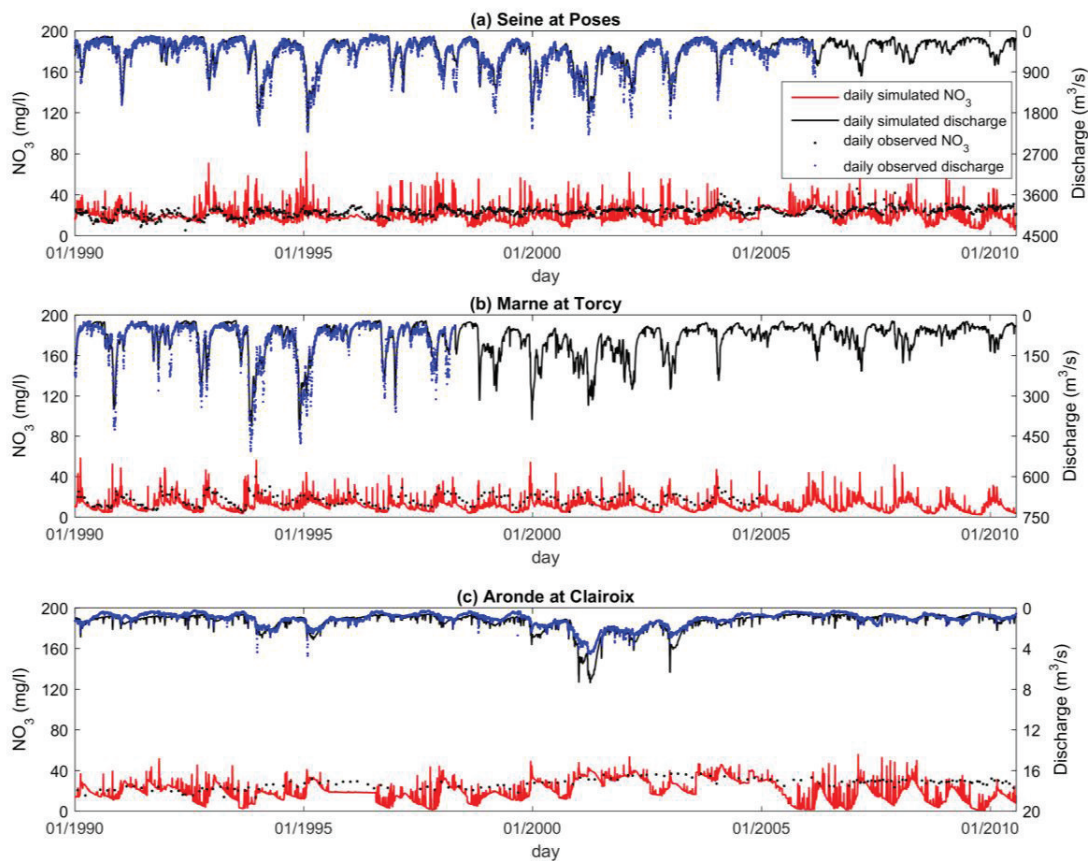


528

529 **Figure 9: Spatial distribution of *KGE* for all stations using point-by-point concurrent comparison.**

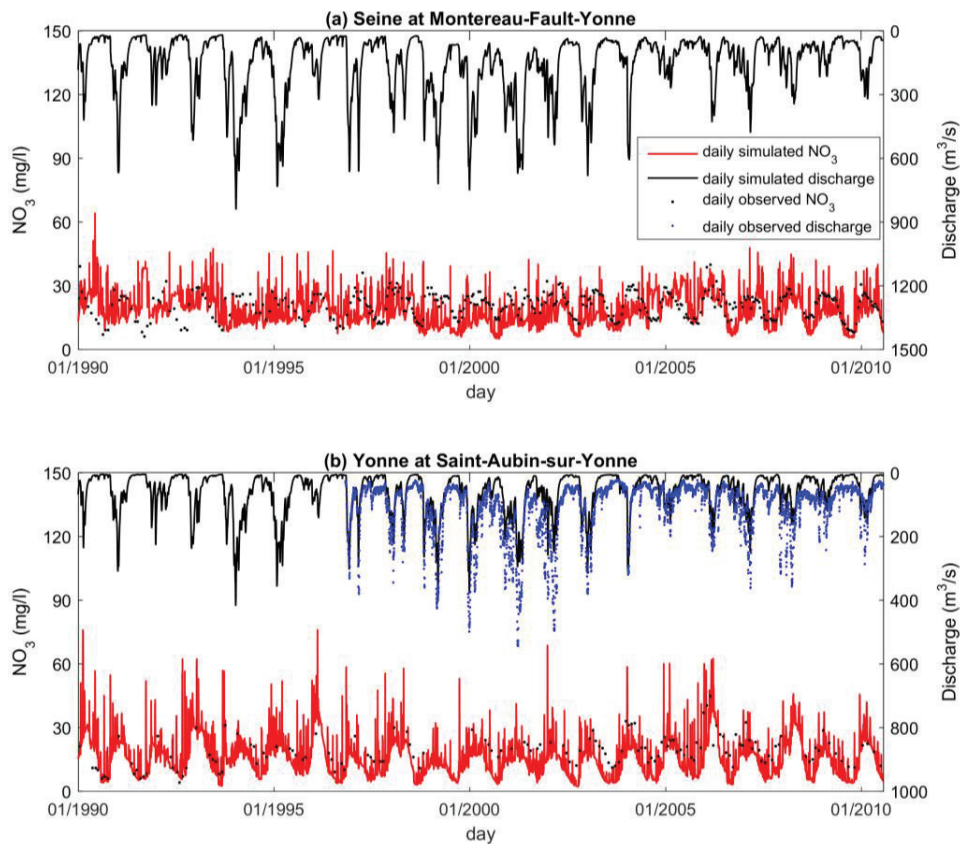
530 Figures 10 and 11 present the comparison between daily observed and simulated nitrate
 531 concentrations at the five selected stations between January 1, 1990 and July 31, 2010. The
 532 model results illustrate that simulated nitrate concentrations tend to follow the inter-annual
 533 variation of observations and hydrographs for the outlet of the basin (the Poses station), Torcy,
 534 Montereau-Fault-Yonne, and Saint-Aubin-sur-Yonne. For those stations, the dynamic simulation
 535 of the nitrate concentration is consistent with the observation (Figures 10 and 11). More
 536 urbanized area can export more nitrate at high flows compared to the low-density suburban area
 537 (Klocher et al., 2009). This case can explain high nitrate concentration at the Poses station which
 538 is downstream of the greater Paris area. Furthermore, this station is downstream of the Seine
 539 River Network with more than fifty percent of agricultural land coverage. The model results for
 540 the Poses station in this study are generally in a good agreement with previous studies. The

541 average nitrate concentration for the dry year (1991) and wet year (2001) are obtained 16.5 mg/l
 542 (359 $\mu\text{mol/l}$) and 20.26 mg/l (440 $\mu\text{mol/l}$). These values are comparable with published results
 543 by Sferratore et al., (2005). The annual average of observation and the Riverstrahler model
 544 (Ducharne et al., 2007) in 2000 are 22.34 and 35 mg/l respectively for the Pose stations. The
 545 mean nitrate concentration of 19.38 mg/l is obtained for the same year in this study. The bias
 546 value (Bias = -0.13 mg/l) is also confirmed the slight underestimation of riverine nitrate
 547 concentration at this station. The reason is likely due to the point sources loadings to the Seine
 548 and Marne Rivers in greater Paris, which were not available for this study.



549 **Figure 10: Comparison of daily simulated and observed nitrate concentration and river discharge:**
 550 **(a) Seine at Poses; (b) Marne at Torcy; and (c) Aronde at Clairoux. Observed discharge data was not**
 551 **available from March 2006 to July 2010 and from July 1998 to July 2010 for Seine at Poses and**
 552 **Marne at Torcy stations, respectively. Observed nitrate data was not available from January 2006**
 553 **to July 2010 for the Marne at Torcy station.**
 554

555 Less accurate nitrate simulations are observed at the Aronde at Clairoux station that has a
556 relatively small drainage area of 285 km² ($KGE = 0.13$ and correlation = 0.42). For the Clairoux
557 station, the model simulated numerous peaks in 2008 (Figure 9c). The summer of 2008 was quite
558 rainy, which explain such peaks. However, the peaks did not appear in the observations, which
559 might be due to the low frequency of the sample analysis. The nitrate concentrations were
560 measured almost monthly (one or two samples per month). This indicates the need for higher
561 spatial resolution modeling to resolve the complex physics at the local scale of the basin, which
562 is an active subject for future research and continuous observation (based on samples
563 conditioned to the river flow). The nitrate concentration at the Aronde at Clairoux station shows
564 high average values. The upstream region of this station is heavily dominated with cropland, thus
565 the emission of the nitrate to river network from this part of the basin is high. Long-term nitrate
566 simulation at Torcy and Saint-Aubin-sur-Yonne stations were simulated with a good accuracy.
567 For the Torcy station $KGE = 0.6$ and correlation = 0.70 were obtained. Similarly, $KGE = 0.45$
568 and correlation = 0.60 were calculated at the Saint-Aubin-sur-Yonne station.
569



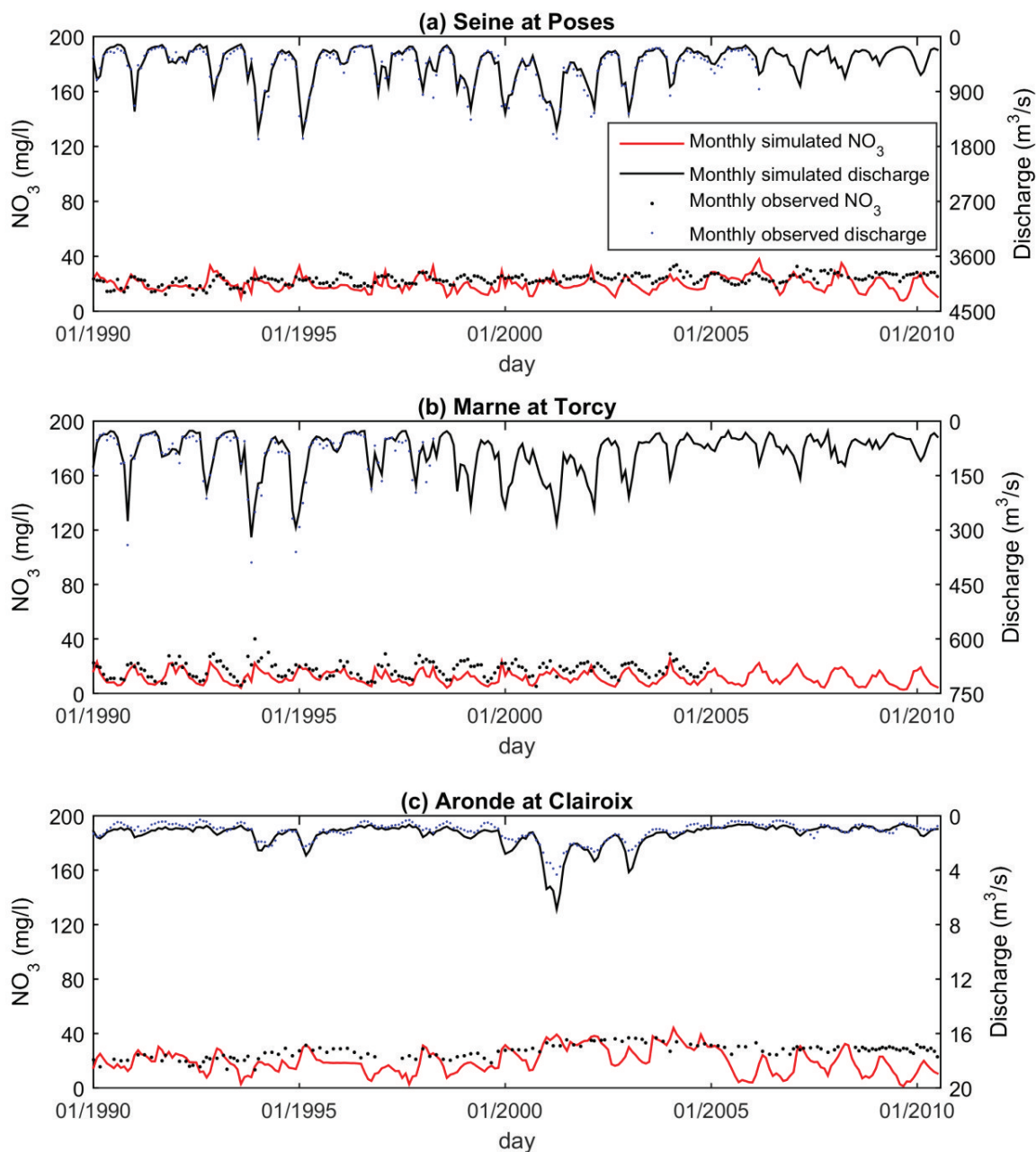
570

571 **Figure 11: Comparison of daily simulated and observed nitrate concentration and river discharge:**
 572 **(a) Seine at Montereau-Fault-Yonne; and (b) Yonne at Saint-Aubin-Sur-Yonne. Observed**
 573 **discharge data was not available for the Seine at Montereau-Fault-Yonne for study time period.**
 574 **Observed nitrate data was not available from January 1990 to October 1996 for the Yonne at Saint-**
 575 **Aubin-sur-Yonne station.**

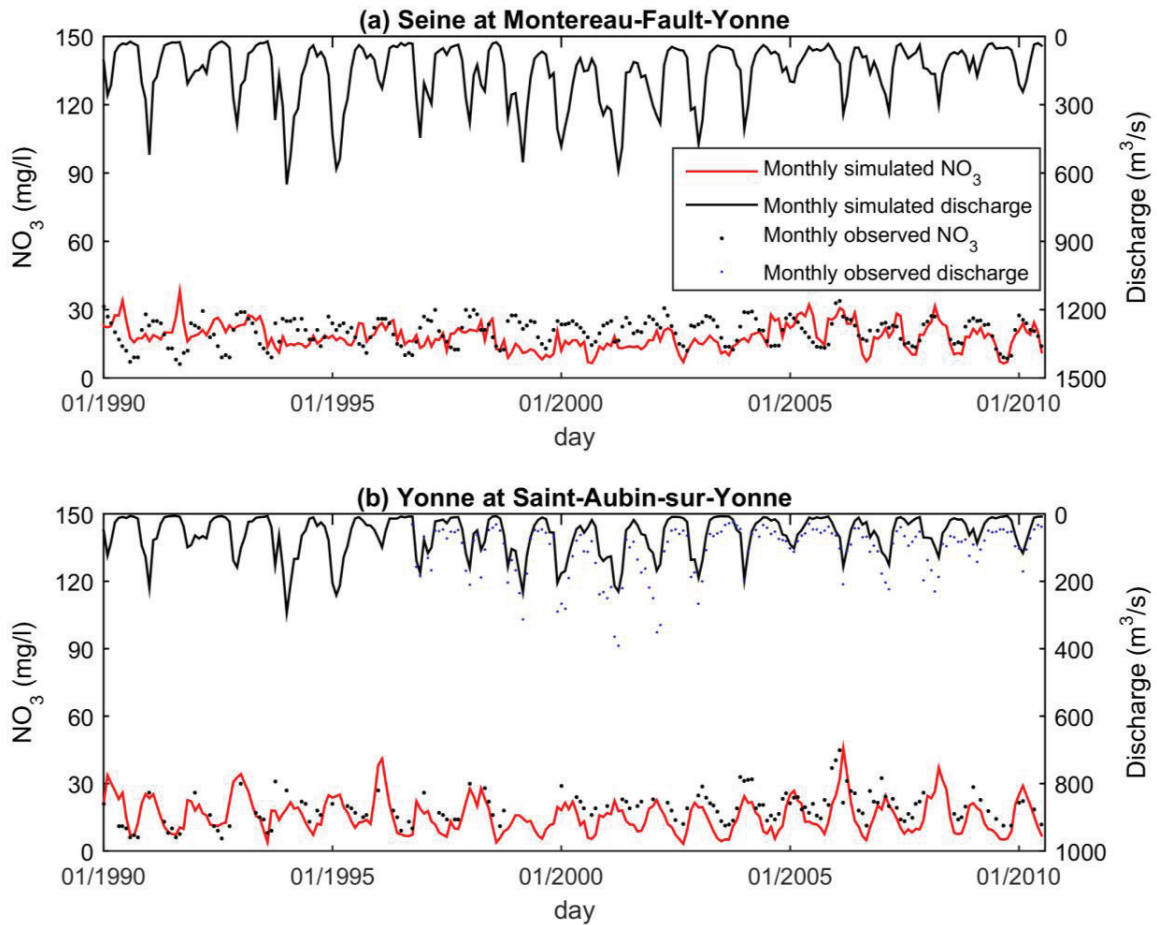
576 Changes in the nitrate concentration are highly affected by the hydrologic simulations. To
 577 have a better representation of variation in nitrate and flow simulations, the seasonal simulations
 578 are also calculated. For this purpose, the daily model results were averaged monthly and the
 579 seasonal comparison was conducted (Figures 12 and 13). A general trend between riverine and
 580 flow simulations can be clearly seen in these figures. Results show that the model captured most
 581 of the seasonal variation of nitrate concentration. Major underestimations of the simulated nitrate
 582 are found during dry season (summer). Such an underestimated simulation is likely due to the
 583 complexity of nitrate attenuation pathways in the groundwater. The discrepancy between

584 observation and simulation can be seen at the the Aronde at Clairoux station. As mentioned
 585 before, this station has less frequent measurements compare to other stations and higher
 586 resolution model for this part of the basin could provide more details.

587

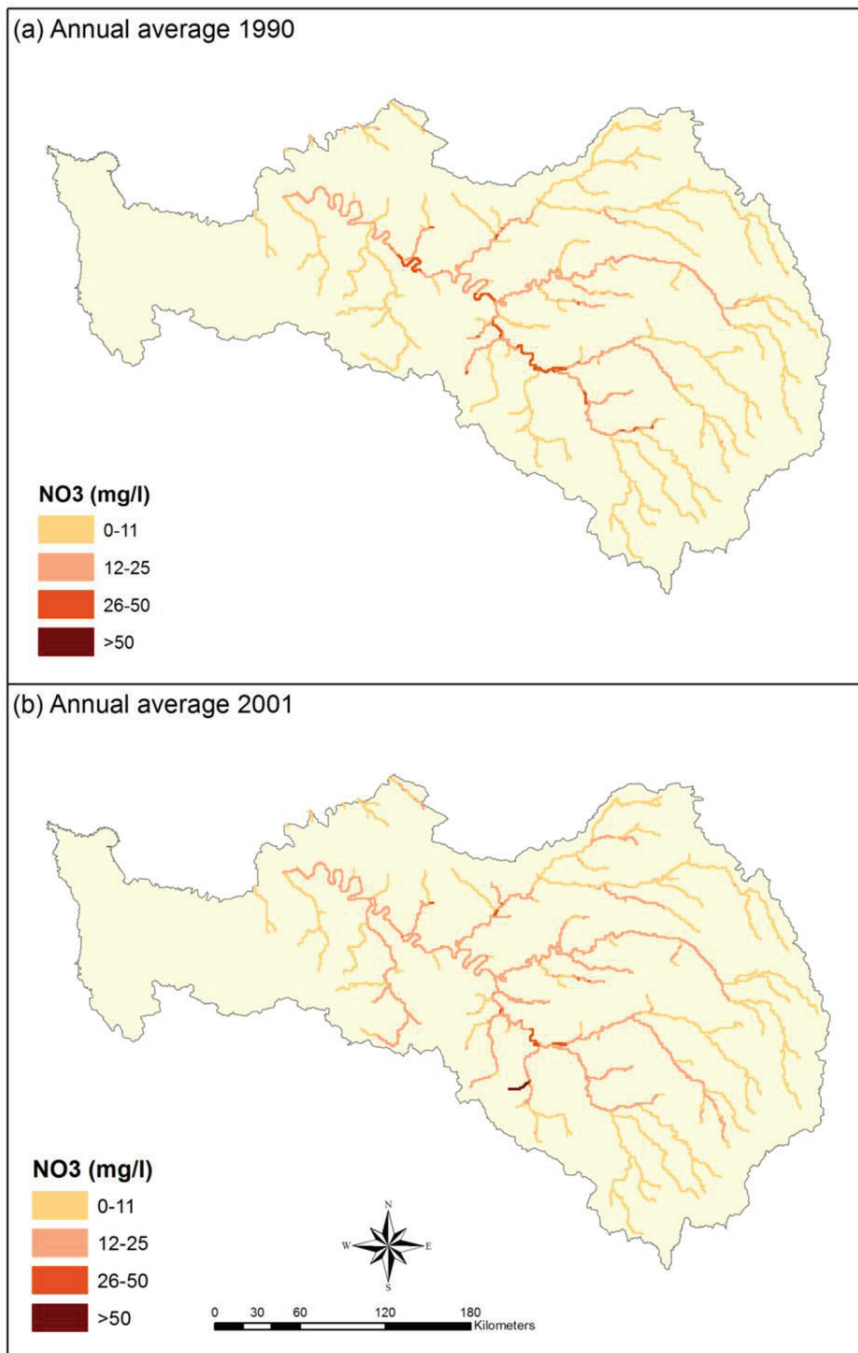


588 **Figure 12: Seasonal comparison of simulated and observed nitrate concentration and river**
 589 **discharge: (a) Seine at Poses; (b) Marne at Torcy; and (c) Aronde at Clairoux.**



590
 591 **Figure 13: Seasonal comparison of simulated and observed nitrate concentration and simulated**
 592 **river discharge: (a) Seine at Montereau-Fault-Yonne; and (b) Yonne at Saint-Aubin-Sur-Yonne.**

593 Figure 14 displays the spatial distribution of riverine nitrate concentration in 1990 (dry
 594 year) and 2001 (wet year). From this figure, the change in nitrate concentration can be
 595 qualitatively assessed for each river cell, which may provide useful information for the regional-
 596 scale nitrate management. For example, comparison of the simulate nitrate concentration
 597 between 1990 and 2001 show that nitrate concentration increases in the south part of the Seine
 598 River Basin (Loing River). The maximum annual nitrate concentration also displays
 599 approximately 60% difference (an increase) comparing a wet year (2001) and a dry year (1990).
 600 Different in-stream nitrate concentration for these years is largely driven by differences in river
 601 water discharge. Annual water yield in 2001 was roughly double as much as in 1990.



602

603 **Figure 14: Spatial variation in nitrate concentration for the Seine River Basin in (a) 1990 and (b)**
 604 **2001.**

605

606 **4-Summary and Perspective**

607 This study describes the implementation of coupled EauDyssée and STICS models to the
608 entire Seine River Basin with total area of 88,000 km². The EauDyssée modeling platform was
609 enhanced to simulate long-term (1971-2010) daily nitrate transport in addition to water transport
610 from surface to rivers and aquifers. The surface and river interactions with aquifers were also
611 considered for the nitrate transport process. The hydraulic variables of river cells such as river
612 flow velocity were computed for the entire basin for the study period. Using the EauDyssée
613 hydrological results, the first order solute transport was developed to simulate riverine nitrate
614 concentration. The spatiotemporal variation of the decay rate was calculated based on the stream
615 order and daily river velocity for river cells. The in-stream nitrate concentration was then
616 simulated for the grid river network (6,481 river cells), which is the backbone of the river routing
617 module of EauDyssée. The simulated in-stream nitrate concentration was calibrated with
618 observations for the selected stations. Simulated groundwater nitrate concentration is comparable
619 to the observation with a bias lower than 10 mg/l in most part of the basin. Comparison of nitrate
620 flux and inflow showed that simulated nitrate is highly dependent on the inflow produced by
621 surface and subsurface waters. Variation of mean annual nitrate from year to year can be
622 explained by the hydrologic regime of that year. Large amount of nitrate flux transports during
623 wet years and less transports during dry years. The long-term simulated nitrate concentration
624 compares favorably to the measured data on a daily basis, especially in the eastern part of the
625 Seine River Basin.

626 The EauDyssée platform has been used by stakeholders and decision makers for more than
627 30 years since its initial MODCOU implementation by Ledoux et al. (1984). The robustness of
628 the EauDyssée platform to simulate complex hydrologic systems with representation of the

629 stream-aquifer exchanges supports the success of the solute transport modeling with the first
630 order approach for riverine nitrate simulation. Hence, this study offers enhanced capabilities for
631 better quantifying water resources and environmental management of Seine River Basin. Long-
632 term computation of flow and nitrate flux may provide a basin-wide comprehensive hydrology
633 and water quality system to study the integration of climate and land surface models with the
634 consideration of rive-aquifer interaction. The outcomes of this study are a good basis for
635 answering needed scientific questions. For instance, this work can provide important
636 perspectives for decision makers focused on the effects of Agri-environment measures and the
637 integration of environmental impacts into the common agricultural policies (Baylis et al., 2008).
638 In addition, this work demonstrates a feasible methodology to quantify the overall variability of
639 the nitrate fluxes in a regional basin stressed by agricultural activities. Furthermore, this coupled
640 framework can be used to project long term climate change effects on nitrate leaching over large-
641 scale basins and to provide stakeholders with tools that quantify the long-term loads and
642 concentration of nitrate (Dirnböck et al., 2016).

643 This study focused on the non-point source pollution and did not include point source
644 pollution sources such as waste water treatment because of data non-availability. Including such
645 data in the modeling framework can improve the estimation of nitrate and the overall bias. Future
646 work can address uncertainty from input data (Thorsen et al., 2001) and model structure using
647 stochastic–deterministic approaches or generalized likelihood uncertainty estimation (GLUE)
648 methodologies (Beven and Binley, 1992).

649 The modeling framework in this study has the flexibility to add or remove nitrate constituents
650 without excessive programming effort. Due to the modeling features and capabilities of the
651 framework presented in this study, this framework can be applied over other basins for water

652 resources and contaminant studies. It offers important perspectives for future large scale
653 applications coupled with existing hydrologic models such as the Soil and Water Assessment
654 Tool (SWAT) (Abbaspour et al., 2015) and the Weather Research and Forecasting-Hydrological
655 (WRF-Hydro) modeling system (Gochis et al, 2015).

656 .

657 **Acknowledgments**

658 This project was partially funded by the French Mines Paristech, French Programme
659 Interdisciplinaire de Recherche sur l’Environnement de la Seine (PIREN-Seine) project, NASA
660 Interdisciplinary Science Project NNX11AJ43G, and USACE Coastal and Hydraulics
661 Laboratory. We are grateful to Dr. Gilles Billen for sharing the water quality data. We kindly
662 thank Ms. Elissa Yeates, Mr. Matthew Crabtree, Mr. Shahab Afshari, and Mr. Charles Wehr for
663 processing observation data and discussion during paper preparation.

664

665

666

667

668

669

670

671

672

673

674

675

676

677

678

679 **References**

- 680 Abbaspour, K.C., E. Rouholahnejad, S. Vaghefi, R. Srinivasan, H. Yang, B. Kløve, 2015. A
681 continental-scale hydrology and water quality model for Europe: Calibration and
682 uncertainty of a high-resolution large-scale SWAT model, *Journal of Hydrology*, 524: 733-
683 752, DOI:10.1016/j.jhydrol.2015.03.027
- 684 Agence de Eau Seine Normandie (AESN), 2013. Etat des Lieux du Bassin de la Seine et des
685 cours d'eau côtiers. [http://www.eau-seine-](http://www.eau-seine-normandie.fr/fileadmin/mediatheque/Politique_de_leau/EDLpost_CB_05122013.pdf/)
686 [normandie.fr/fileadmin/mediatheque/Politique_de_leau/EDLpost_CB_05122013.pdf/](http://www.eau-seine-normandie.fr/fileadmin/mediatheque/Politique_de_leau/EDLpost_CB_05122013.pdf/)
687 (accessed 04/18/2017)
- 688 Alexander Richard B., P. J. Johnes, E. W. Boyer, R. A. Smith, 2002. A comparison of models for
689 estimating the riverine export of nitrogen from large watersheds. *Biogeochemistry* Springer,
690 57/58: 295–339
- 691 Arnold, J.G., R. Srinivasan, R.S. Muttiah, P.M. Allen, 1999. Continental scale simulation of the
692 hydrologic balance, *Journal of the American Water Resources Association*, 35 (5): 1037-
693 1051
- 694 Baratelli, F., N. Flipoa, F. Moatar, 2016. Estimation of stream-aquifer exchanges at regional
695 scale using a distributed model: Sensitivity to in-stream water level fluctuations, riverbed
696 elevation and roughness, *Journal of Hydrology*, 542: 686-703, DOI:
697 10.1016/j.jhydrol.2016.09.041

698 Baylis, K., S. Peplow, G. Rausser, L. Simon, 2008. Agri-environmental policies in the EU and
699 United States: A comparison, *Ecological Economics*, 65 (4): 753-764,
700 DOI:10.1016/j.ecolecon.2007.07.034

701 Beaudoin, N., N. Gallois, P. Viennot, C. Le Bas, T. Puech, C. Schott, S. Buis, B. Mary, 2016.
702 Evaluation of a spatialized agronomic model in predicting yield and N leaching at the scale
703 of the Seine-Normandie Basin, *Environmental Science and Pollution Research*, 1-30,
704 DOI:10.1007/s11356-016-7478-3

705 Bennett, N. D., B.F.W. Croke, G. Guariso, J.H.A. Guillaume, S.H. Hamilton, A.J. Jakeman, S.
706 Marsili-Libelli, L.T.H. Newham, J.P. Norton, C. Perrin, S.A. Pierce, B. Robson, R. Seppelt,
707 A.A. Voinov, B.D. Fath, V. Andreassian, 2013. Characterising performance of
708 environmental mode. *Environmental Modelling & Software*. 40:1-20,
709 DOI:10.1016/j.envsoft.2012.09.011

710 Beven, K. A., Binley, 1992. The future of distributed models: model calibration and uncertainty
711 prediction. *Hydrological processes*, 6(3): 279-298

712 Billen, G., J. Garnier, J. Nemery, M. Sebilo, A. Sferratore, P. Benoit, S. Barles, M. Benoit, 2007.
713 A long-term view of nutrient transfers through the Seine river continuum. *Science of the*
714 *Total Environment*, 375: 80-97, DOI:10.1016/j.scitotenv.2006.12.005

715 Borah D, M. Bera, 2003. Watershed-scale hydrologic and nonpoint-source pollution models:
716 Review of mathematical bases. *Transactions of the ASAE* 46(6): 1553–1566.

717

718 Bourgois, C., P.-A. Jayet, , F. Habets, P. Viennot, 2016. Estimating the marginal social value of
719 agriculturally driven nitrate concentrations in an aquifer: A Combined theoretical-applied
720 approach. *Water Economics and Policy*, 1650021, DOI:10.1142/S2382624X16500211.

721 Brisson, N., R. Francoise, G. Philippe, J. Loreou, B. Nicoullaud, N., X. Tayot, D. Plénet, MH.
722 Jeuffroy, A. Bouthier, D. Ripoche, B. Mary, E. Justes, 2002. STICS : a generic model for
723 simulating crops and their water and nitrogen balances . II . Model validation for wheat and
724 maize. *Agronomie* 22, 69-92, DOI:10.1051/agro: 2001005

725 Brisson, N., C. Gary, E. Justes, R. Roche, B. Mary, D. Ripoche, D. Zimmer, J. Sierra, P.
726 Bertuzzi, P. Burger, F. Bussièrè, Y.M. Cabidoche, P. Cellier, P. Debaeke, J.P. Gaudillère,
727 C. Hénault, F. Maraux, B. Seguin, H. Sinoquet, 2003. An overview of the crop model
728 STICS. *European Journal of Agronomy* 18(3-4): 309-332, DOI: 10.1016/S1161-
729 0301(02)00110-7

730 Brisson, N., B. Mary, D. Ripoche, M.H. Jeuffroy, F. Ruget, B. Nicoullaud, P. Gate, F. Devienne-
731 Barret, R. Antonioletti, C. Durr , 1998. STICS: a generic model for the simulation of crops
732 and their water and nitrogen balances. I. Theory and parameterization applied to wheat and
733 corn. *Agronomie* 18(5-6): 311-346, DOI: 10.1051/agro:19980501

734 Contoux, C., S. Violette, R. Vivona, P. Goblet, D. Patriarche, 2013. How basin model results
735 enable the study of multi-layer aquifer response to pumping: the Paris Basin, France.
736 *Hydrogeology Journal*, 21(3): 545-557, DOI:10.1007/s10040-013-0955-6

737 Cugier, P., G. Billen, J.F. Guillaud, J. Garnier, A. Ménesguen, 2005. Modelling the
738 eutrophication of the Seine Bight (France) under historical, present and future riverine
739 nutrient loading. *Journal of Hydrology*, 304, 381-396, DOI:10.1016/j.jhydrol.2004.07.049

740 Daniel E.B., J.V. Camp, E.J. LeBoeuf, J.R. Penrod, J.P. Dobbins, M.D. Abkowitz, 2011.
741 Watershed Modeling and its Applications: A State-of-the-Art Review. *The Open Hydrology*
742 *Journal*, 5: 26–50.

743 David, C.H., F. Habets, D.R. Maidment, Z.-L. Yang, 2011a. RAPID Applied to the SIM-France
744 Model. *Hydrological Processes*, 25(22):3412-3425, DOI: 10.1002/hyp.8070

745 David, C.H., D.R. Maidment, G.-Y. Niu, Z.-L. Yang, F. Habets, V. Eijkhout, 2011b. River
746 network routing on the NHDPlus dataset. *Journal of Hydrometeorology*, 12:913-934,
747 DOI:10.1175/2011JHM1345.1

748 David, C.H., Z.-L. Yang, S. Hong, 2013. Regional-scale river flow modeling using off-the-shelf
749 runoff products, thousands of mapped rivers and hundreds of stream flow gauges.
750 *Environmental Modelling & Software*, 42:116-132, DOI:10.1016/j.envsoft.2012.12.011

751 De Wit, M., H. Behrendt, G. Bendoricchio, W. Bleuten, P. van Gaans, 2002. The contribution of
752 agriculture to nutrient pollution in three European rivers , with reference to the European
753 Nitrates Directive. *European Water Management Online*, official publication of the
754 European Water Association (EWA). http://www.ewaonline.de/journal/2002_02.pdf/
755 (accessed 04/18/2017)

756 Deschesnes, J., J.-P. Villeneuve, E. Ledoux, G. Girard, 1985. Modeling the hydrologic cycle: the
757 MC model. Part I - principles and description. *Nordic Hydrology*, 16(5), 257-272

758 Dirnböck, T., J. Kobler, D. Kraus, R. Grote, R. Kiese, 2016. Impacts of management and climate
759 change on nitrate leaching in a forested karst area, *Journal of Environmental Management*,
760 165:243-252, DOI:10.1016/j.jenvman.2015.09.039

761 Ducharne A, 2008. Importance of stream temperature to climate change impact on water quality,
762 *Hydrology and Earth System Sciences*, 12:797-810

763 Ducharne A, Baubion C, Beaudoin N, Benoit M, Billen G, Brisson N, et al., 2007. Long term
764 prospective of the Seine river system: Confronting climatic and direct anthropogenic
765 changes. *Science of the Total Environment*, 375(1-3):292–311,
766 DOI:10.1016/j.scitotenv.2006. 12.011

767 Durand, Y., E. Brun, L. Merindol, G. Guyomarch, B. Lesaffre, E. Martin, 1993, A
768 meteorological estimation of relevant parameters for snow models, *Annals of Glaciology*,
769 18(1):65-71, DOI: 10.3198/1993AoG18-1-65-71

770 Ensign, S. H., M. W. Doyle, 2006. Nutrient spiraling in streams and river networks. *Journal of*
771 *Geophysical Research*, 111, G04009, DOI:10.1029/2005JG000114

772 Even, S., G. Billen, N. Bacq, S. Théry , D. Ruelland, J. Garnier, P. Cugier, M. Poulin, S. Blanc,
773 F. Lamy, C. Paffoni, 2007. New tools for modelling water quality of hydrosystems: an
774 application in the Seine River basin in the frame of the Water Framework Directive.
775 *Science of the Total Environment*, 375:274-291, DOI:10.1016/j.scitotenv.2006.12.019

776 Faulkner, B.R., M.E. Campana, 2007. Compartmental model of nitrate retention in streams.
777 Water Resources Research, 43, W02406, DOI:10.1029/2006WR004920

778 Flipo, N., S. Even, M. Poulin, S. Théry, E. Ledoux, 2007a. Modeling nitrate fluxes at the
779 catchment scale using the integrated tool CAWAQS. Science of the Total Environment,
780 375, 69-79, DOI:10.1016/j.scitotenv.2006.12.016

781 Flipo, N., N. Jeannée, M. Poulin, S. Even, E. Ledoux, 2007b. Assessment of nitrate pollution in
782 the Grand Morin aquifers (France): combined use of geostatistics and physically based
783 modeling. Environmental Pollution, 146, 241-256, DOI:10.1016/j.envpol.2006.03.056

784 Flipo, N. A. Mouhri, B. Labarthe, S. Biancamaria, A. Rivière, P. Weill, 2014. Continental
785 hydrosystem modelling: the concept of nested stream-aquifer interfaces. Hydrology and
786 Earth System Sciences 18:3121–3149, DOI: 10.5194/hess-18-3121-2014

787 Follum, M.L., A.A. Tavakoly, J.D. Niemann, A.D. Snow, 2016. AutoRAPID: A model for
788 prompt streamflow estimation and flood inundation mapping over regional to continental
789 extents. Journal of the American Water Resources Association, 1-20, DOI: 10.1111/1752-
790 1688.12476

791 Galloway J. N., F.J. Dentener, D.G. Capone, et al. 2004. Nitrogen Cycles: Past, Present, and
792 Future. Biogeochemistry 70(2): 153–226, DOI:10.1007/s10533-004-0370-0

793 Garnier, J., G. Billen, G. Vilain, A. Martinez, M. Silvestre, E. Mounier, F. Toche, 2009. Nitrous
794 oxide (N₂O) in the Seine river and basin: Observations and budgets. Agric. Ecosyst.
795 Environ. DOI: 10.1016/j.agee.2009.04.024

796 Garnier, J., J. Némery, G. Billen, S. Théry, 2005. Nutrient dynamics and control of
797 eutrophication in the Marne River system: modelling the role of exchangeable phosphorus.
798 Journal of Hydrology, 304:397-412, DOI:10.1016/j.jhydrol.2004.07.040

799 Gochis, D.J., W. Yu, D.N. Yates, 2015. The WRF-Hydro Model Technical Description and
800 User's Guide, Version 3.0. NCAR Technical Document, 120 pp.
801 http://www.ral.ucar.edu/projects/wrf_hydro/ (accessed 04/20/2017)

802 Golaz-Cavazzi, C., P. Etchevers, F. Habets, E. Ledoux, J. Noilhan, 2001. Comparison of two
803 hydrological simulations of the Rhone basin. Physics and Chemistry of the Earth, Part B:
804 Hydrology, Oceans and Atmosphere, 26(5-6):461-466, DOI: 10.1016/S1464-
805 1909(01)00035-1

806 Gomez, E., E. Ledoux, J. Monget, G.De. Marsily, 2003a. Distributed surface-groundwater
807 coupled model applied to climate or long term water management impacts at basin scale.
808 European Water, 3-8

809 Gomez, E., E. Ledoux, P. Viennot, C. Mignolet, M. Benoit, C. Bornerand, C. Schott, B. Mary, G.
810 Billen, A. Ducharne, D. Brunstein, 2003b. Un outil de modélisation intégrée du transfert des
811 nitrates sur un système hydrologique: application au bassin de la seine. La Houille Blanche,
812 3:38-45, DOI:10.1051/lhb/2003045

813 Grizzetti B., P. Passy, G. Billen, F. Bouraoui, J. Garnier, L. Lassaletta, 2015. The role of water
814 nitrogen retention in integrated nutrient management: assessment in a large basin using
815 different modelling approaches. Environmental Research Letter, 10(6):065,008,
816 DOI:10.1088/1748-9326/10/6/065008

817 Gupta, H.V., H. Kling, K.K. Yilmaz, G.F. Martinez, 2009. Decomposition of the mean squared
818 error and NSE performance criteria: Implications for improving hydrological modelling.
819 Journal of Hydrology, 377:80-91, DOI:10.1016/j.jhydrol.2009.08.003

820 Haas, M.B., B. Guse, M. Pfannerstill, N. Fohrer, 2016. A joined multi-metric calibration of river
821 discharge and nitrate loads with different performance measures. Journal of Hydrology,
822 536:534-545, DOI:10.1016/j.jhydrol.2016.03.001

823 Habets, F., A. Boone, J.L. Champeaux, P. Etchevers, L. Franchiste'guy, E. Leblois, E. Ledoux,
824 P. Le Moigne, E. Martin, S. Morel, J. Noilhan, P. Quintana Segui', F. Rousset-Regimbeau,
825 P. Viennot, 2008. The SAFRAN-ISBA-MODCOU hydrometeorological model applied over
826 France. Journal Geophysical Research, 113:1-18, DOI:10.1029/2007JD008548

827 Habets F., J. Boé, M. Déqué, A. Ducharne, S. Gascoin, A. Hachour, E. Martin, C. Pagé, E.
828 Sauquet, L. Terray, D. Thiéry, L. Oudin, P. Viennot, 2013. Impact of climate change on the
829 hydrogeology of two basins in Northern France, Climatic Change, 121(4): 771-785, DOI:
830 10.1007/s10584-013-0934-x

831 Hooda, P.S., M. Moynagh, I.F. Svoboda, M. Thurlow, M. Stewart, M. Thomson, H.A. Anderson,
832 1997. Streamwater nitrate concentrations in six agricultural catchments in Scotland. Science
833 of The Total Environment, 201(1):63-78, DOI:10.1016/S0048-9697(97)84053-3

834 Kampas, A., B. White, 2003. Probabilistic programming for nitrate pollution control: Comparing
835 different probabilistic constraint approximations. European Journal of Operational
836 Research, 147(1):217-228, DOI:10.1016/S0377-2217(02)00254-0

837 Klockner, C.A., S.S. Kaushal, P.M. Groffman, P.M. Mayer, R.P. Morgan, 2009. Nitrogen uptake
838 and denitrification in restored and unrestored streams in urban Maryland, USA. *Aquatic*
839 *Sciences*, 71:411–424, DOI 10.1007/s00027-009-0118-y

840 Kunkel, R., M. Bach, H. Behrendt, F. Wendland, 2004. Groundwaterborne nitrate intakes into
841 surface waters in Germany. *Water Science Technology* 49(3):11–19

842 Kunkel, R., F. Herrmann, H.-E. Kape, L. Keller, F. Koch, B. Tetzlaff, F. Wendland, 2017.
843 Simulation of terrestrial nitrogen fluxes in Mecklenburg- Vorpommern and scenario
844 analyses how to reach N-quality targets for groundwater and the coastal waters.
845 *Environmental Earth Science* 76:146: DOI 10.1007/s12665-017-6437-8

846 Kunkel R, F. Wendland, 1997. WEKU - a GIS-supported stochastic model of groundwater
847 residence times in upper aquifers for the supraregional groundwater management. *Environ*
848 *mental Geology* 30(1–2):1-9

849 Kunkel R, F. Wendland, 2002. The GROWA98 model for water balance analysis in large river
850 basins-the river Elbe case study. *Journal of Hydrology* 259(1–4):152–162

851 Landreau, A., J.C. Roux, 1984. Répartition et évolution des teneur en nitrates dans les eaux
852 souterraines en France. Note technique au BRGM, 84 ENV 002.

853 Ledoux, E., G. Girard, J.P. Villeneuve, 1984. Proposition d'un modèle couplé pour la simulation
854 conjointe des écoulements de surface et des écoulements souterrains sur un bassin
855 hydrologique. *La Houille Blanche*, 101-110.